JOURNAL OF GUIDANCE, CONTROL, AND DYNAMICS
Vol. 22, No. 6, November–December 1999

Feedback Control for Slew Maneuver Using On–Off Thrusters

Hyochoong Bang,* Youngwoong Park,† and Jungyoup Han†
Korea Aerospace Research Institute, Daejon 305-600, Republic of Korea
and
Han Hwangbo‡
Korea Telecom, Seoul 143-191, Republic of Korea

A new output-feedback control approach for the single-axis rotational maneuver of a flexible structure by use of on–off thrusters is discussed. The target structural model represents a large-space-structure type with relatively low natural frequencies. The large overshoot induced by phase error of the applied torque input is minimized by the new control law. The thruster output is modulated in pulse width so that the output profile is similar to continuously smoothed control histories. The main idea of the new controller is based on a closed-loop switching function that is constructed from a near-minimum-time output-feedback tracking control law. The proposed control law has advantages of robustness as an output-feedback law as well as enhanced performance for the slew maneuver of flexible structures by use of on–off actuators.

I. Introduction

THE single-axis slew maneuver of flexible space structures has received significant attention in many previous studies.[1–6] The application areas are also very diverse, and there are a number of control approaches. The flexible-structure model is typically represented by a center rigid hub to which a flexible appendage is attached, simulating solar arrays and antennas of spacecraft. The actuators are attached to the center hub and/or flexible appendage.

An important element for the slew maneuver strategy is the type of actuators. The actuators are divided into a discrete on–off type with a fixed output level[7–20] and a continuous type with a time-varying output.[21–23] Strictly on–off actuators such as spacecraft thrusters are usually applied to the minimum-time slew maneuver.[9–12] The on–off actuators in turn cause a residual vibration problem, creating abrupt changes of vibrational energy during the maneuver. An exemplary time optimal control strategy is to find switching times based on the finite mathematical model of the flexible structure. The switching times are parameterized to satisfy terminal boundary conditions such as residual vibration energy and desired angular displacement.[9–13,19] Liu and Wie[10] and Wie et al.[11,13] applied the switching-time optimization technique to compute the switching times that satisfy additional robustness conditions. This approach partially solves the robustness issue of switching times with respect to the modeling uncertainties. One potential drawback of the switching-time approach lies still in modeling uncertainties and the associated maneuver performance. Other approaches that generate thruster profiles are available,[14–16] and some of them include various performance objectives such as minimum fuel/time and vibrational energy.[17–19]

The actuator is another source of uncertainty because the thrusters do not ideally operate in on–off fashion. The open-loop nature of switching times makes the practical implementation of the control technique rather difficult. A direct output feedback without switching-time parameterization is reported in Ref. 20 (and other papers, obviously). This control law is a minimum-time closed-loop switching law based on the approximated pure rigid-body dynamics. Even though the control law itself is not exactly minimum time in principle because of the approximation, the output-feedback control law proved satisfactory in performance. Experimental verifications were also conducted for the validation of the proposed control law in Ref. 20.

Another representative actuator type is a continuous output device. The most distinct example of this type is a reaction wheel that uses a servomotor. For this type of actuator, many control strategies have been proposed in conjunction with finite approximations of dynamic models.[3–6] The control torque profiles are usually time varying and adjusted to satisfy various terminal constraints.[5] Modeling uncertainties are handled by robust control algorithms applied to linear finite-dimensional systems.[5,6] Also, the direct output-feedback control has experienced considerable progress because of inherent advantages. Examples of output feedback are reported in Refs. 21–23. Fuji et al. proposed an output-feedback control law for the slew maneuver based upon the hub angle information as well as internal reaction torque at the root of the hub.[22] The reaction wheel actuator and minimum-time slew maneuver strategy are combined together in Ref. 23 to lead to the so-called near-minimum-time control strategy. The central idea is a globally stabilizing output-feedback law based on the Lyapunov stability theory and reference target trajectories. The precomputed smoothed reference motions are used to generate a feedback tracking control command. The experimental verification for this approach is also presented in Ref. 23. Obviously there are a number of other strategies reported elsewhere for the similar subject that are not included in this paper because of limited space.

Despite advantages of continuous actuation devices, the on–off actuator is still widely adopted as a principal actuator in spacecraft attitude maneuver and control. There are practical situations in which the slew maneuver of a large flexible spacecraft needs to be implemented by on–off thrusters. Discontinuity of the actuator output may excite the flexibility and result in degradation of pointing performance. This problem has been indirectly solved by structural filter design and inherent structural damping in practical situations. In this paper we present analysis results on a new slew maneuver strategy by use of on–off actuators. This approach is essentially a combination of the output feedback by use of on–off thrusters, as in Ref. 20, and the near-minimum-time tracking control law with a reaction wheel actuator, as in Ref. 23. The smoothed reference maneuver is converted into a pulse-width modulation (PWM) signal to adjust the thruster pulse width, thus trying to preserve the original smoothing effect even though the PWM output itself is still discontinuous. The modulation of the thruster pulse width is in particular targeted to reduce the overshoot and residual vibration caused by the flexibility of the structure. Special focus is placed on a structure model with low natural frequencies, which is a usual characteristic of typical large space structures. The open-loop PWM is also extended into the modulation of a closed-loop tracking signal. This naturally improves the pointing

Received 10 September 1998; revision received 26 April 1999; accepted for publication 30 April 1999.

*Senior Research Scientist, P.O. Box 113, Space Division, Yusung-Gu. Member AIAA.
†Research Scientist, P.O. Box 113, Space Division, Yusung-Gu.
‡Executive Vice President, Gwang Jin-Gu. Associate Fellow AIAA.

performance in the presence of unknown disturbance and parameter uncertainty.

The control law proposed in this study provides an example of using on–off actuators to build a smoothed torque profile. The discrete on–off actuator output is therefore tailored to meet the requirement of the smoothed control command to the extent limited by the nature of the thruster actuators.

II. Dynamics and Maneuver Description

The slewing motion of a rigid hub with a flexible appendage attached to the hub is graphically presented in Fig. 1. We consider the rotational motion only without any translation of the center of mass of the whole structure.

The center rotation is denoted as θ, and the deflection of the appendage is represented by $w(x, t)$. It is assumed that the control torque is applied to the rigid hub only. The governing equations of motion for the flexible structure are derived as[22,23]

$$I_c\frac{\mathrm{d}^2\theta}{\mathrm{d}t^2}+\int_{l_0}^{l}\rho x\left(x\frac{\mathrm{d}^2\theta}{\mathrm{d}t^2}+\frac{\partial^2 w}{\partial t^2}\right)\mathrm{d}x+m_t l\left(l\frac{\mathrm{d}^2\theta}{\mathrm{d}t^2}+\frac{\partial^2 w}{\partial t^2}\bigg|_l\right)=u \tag{1}$$

$$\rho\left(\frac{\partial^2 w}{\partial t^2}+x\frac{\mathrm{d}^2\theta}{\mathrm{d}t^2}\right)+\mathrm{EI}\frac{\partial^4 w}{\partial x^4}=0 \tag{2}$$

where I_c represents the moment of inertia of the center hub, ρ is the linear mass density of the appendage, EI is the elastic rigidity of the appendage, m_t is the tip mass, l is the length from the center to the appendage tip, and u is the torque applied by the actuator located at the center hub. The boundary conditions are given geometrically at the root and the natural boundary condition at the tip of the appendage.[23] The actuator as discussed so far is assumed to be an on–off actuator with output level of 1 N · m.

The material properties and first five natural frequencies computed by the finite-element method are provided in Table 1. The first flexible-mode natural frequency is 0.67 Hz, like that of a typical large-space-structure model. As it will be shown in the simulation result of Fig. 2 in Sec. III, the first mode is a dominant mode excited by the actuator level applied. The low-frequency structure exhibits considerable dynamic interaction between the appendage and the center hub in terms of the magnitude of appendage deflection. The control torque level is another element that determines the maneuver performance. The smaller control torque level results in a longer settling time, and the input torque profile needs to be selected judiciously to minimize the potential phase error between the control input and the hub response.

Table 1 Material properties and natural frequencies

Properties	Value	Natural frequencies, Hz
Linear mass density, ρ	0.542 kg/m	0.000
Elastic rigidity, EI	4.593 N · m^2	0.673
Tip mass, m_t	0.20 kg	3.788
Moment of inertia of hub, I_c	2.32 kg · m^2	12.94
Appendage length, l	1.5 m	33.84
Hub radius, l_0	0.4 m	——

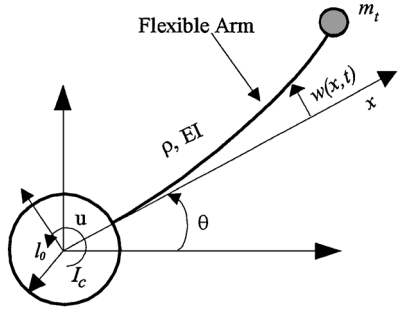

Fig. 1 Flexible-structure model and parameter notations.

The objective of the slew maneuver of this study is a rest-to-rest maneuver, as with other previous studies. The whole structure is rotated about the vertical axis from a rest state to another rest state in the shortest time possible. The angular-displacement change is arbitrarily set to be 40 deg throughout this study. Vibration suppression should be conducted in parallel with the slew maneuver in order to achieve the final rest condition as quickly as possible. The sensor output available for the output feedback is hub angle θ and angular rate $\dot{\theta}$, and no state estimator is involved. The control law itself is largely concentrated on the feedback control by on–off thrusters. As mentioned in Sec. I, the near-minimum-time feedback tracking control law in Ref. 23 is taken as the principal motivation of this study. The smoothed reference motion is reconfigured to be suitable to application in on–off thrusters.

III. Output-Feedback Controller Design

Before we attempt to design the principal control law of this study, the application of a typical closed-loop feedback control strategy is made.[20,24] This will provide a fundamental motivation for this study by disclosing the nature of the problem.

Minimum-Time Maneuver

The minimum-time controller is well known to be a bang-bang for a simple rigid body.[24] The single switching takes place at the half-maneuver time. The control law also can be constructed in a feedback form, that is, for a pure rigid body

$$I\ddot{\theta}=u \tag{3}$$

The closed-loop minimum-time feedback control law is[24]

$$u(t)=-N\,\mathrm{sign}[\theta-\theta_f+(I/2N)\dot{\theta}|\dot{\theta}|] \tag{4}$$

where N is the magnitude of the maximum applied torque and sign(f) (1 if $f>0$ and -1 if $f<0$) is a sign function determining the control torque direction. The control law of Eq. (4) possesses the advantages of feedback control law handling modeling uncertainty and initial condition error. Now to apply the same control law to the flexible-structure slewing motion, the governing equations of Eqs. (1) and (2) are approximated into a pure rigid body. In other words,

$$I_{\mathrm{tot}}\ddot{\theta}=u \tag{5}$$

where I_{tot} is the moment of inertia of the whole structure at the undeformed state. Mathematically,

$$I_{\mathrm{tot}}=I_c+\int_{l_0}^{l}\rho x^2\,\mathrm{d}x+m_t l^2 \tag{6}$$

In Ref. 20 a minimum-time controller design based on the approximated pure rigid-body dynamics is demonstrated with experimental results. The feedback control law now simply becomes

$$u(t)=-N\,\mathrm{sign}[\theta-\theta_f+(I_{\mathrm{tot}}/2N)\dot{\theta}|\dot{\theta}|] \tag{7}$$

where θ_f is the final desired angle to be reached. The above control law is directly applied to the coupled rigid and flexible dynamic equations of motion in Eqs. (1) and (2). Now a natural question arises as to the accuracy of the approximated model and the performance with the corresponding controller applied. One key element to be taken into account in this question is the natural frequencies of the flexible modes. If the natural frequencies of the flexible model are relatively high, then the rigid body approximation may well describe the original dynamics. However, if the natural frequencies are relatively low, as of a typical aspect of large space structures, then the approximated dynamics may not sufficiently reflect the original dynamics. Another factor of importance is the actuator output level. If the actuator output level is high enough, the flexibility effect can be effectively handled by the control authority available.

Sample simulation results based on the closed-loop minimum-time control law are presented in Fig. 2. Hub angles and angular rate as well as actuator response are plotted together. For consideration of fuel expenditure, a deadband is activated to limit thruster firings within a certain pointing accuracy band.

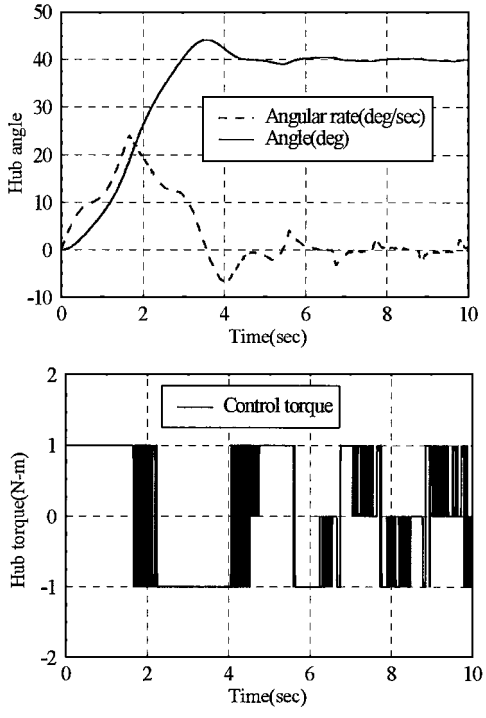

Fig. 2 Minimum-time simulation results with the feedback control law.

As one can see in Fig. 2, an overshoot in the hub angle is a result of the control law's using pure rigid dynamics. Also, it is worthwhile to note that the maneuver profile is asymmetric during the minimum maneuver time, which is given by[22,24]

$$t_f = \sqrt{\frac{4I_{\text{tot}}(\theta_f - \theta_0)}{N}} \tag{8}$$

which is equal to 3.45 s in this case. Convergence to the final desired angle is achieved after the minimum maneuver time. Also, multiple firings are observed around the half-maneuver time, analogous to that of open-loop approaches in Refs. 9–12. The excessive overshoot in the hub angle is attributed to the error caused by the pure rigid-body approximation. This is also due to the phase error by the multiple firings, which do not satisfy the exact minimum-time rest-to-rest maneuver condition.[9–12] Thus the simple rigid-body approximation and closed-loop control law may not be adequate for the desired slew objective.

On the other hand, Agrawal and Bang[20] investigated a somewhat different output-feedback control law by introducing an additional design parameter into the control law as

$$u(t) = -N \operatorname{sign}[\theta - \theta_f + \gamma(I_{\text{tot}}/2N)\dot{\theta}|\dot{\theta}|] \tag{9}$$

The parameter $\gamma > 0$ is adjusted to arrive at satisfactory time responses. It turns out that γ plays the role of a derivative feedback gain as it appears in front of the angular velocity ($\dot{\theta}$) term. The above control law and a deadband to minimize fuel consumption was directly implemented for the experimental verification by use of a ground-based hardware simulator.[20]

Tracking Control Law

In the preceding subsection, it was shown that the approximated rigid dynamics are not appropriate for the minimum-time rest-to-rest maneuver. In particular for the structural model with a low first natural frequency, large overshoot resulted. The overshoot is attributed to the phase error caused by the multiple firings around the half-maneuver time. It is evident that the phase error is directly related to the characteristics of the original flexible dynamics and the simplified modeling.

The problem of minimum-time feedback control law is viewed from a different perspective. The multiple firings around the half-maneuver time are shifted when a different switching function is attempted. The new switching function is motivated by the feedback tracking control law of Ref. 23. The output-feedback tracking control law based on a priori reference trajectories is described as[23]

$$u(t) = u_{\text{ref}} - [g_1(\theta - \theta_{\text{ref}}) + g_2(\dot{\theta} - \dot{\theta}_{\text{ref}})] \tag{10}$$

where $g_1 > 0$ and $g_2 > 0$ are constant design parameters and the reference control torque u_{ref} corresponds to a shaped bang-bang control torque profile. The sharp change of control sign is minimized by a smoothed shaping technique. The mathematical expression of u_{ref} is given as

$$u_{\text{ref}}(t) = I_{\text{tot}}\ddot{\theta}_{\text{ref}} = Nf(t, \Delta t) \tag{11}$$

where the shaping function $f(t, \Delta t)$ is mathematically represented as

$$f(t, \Delta) = \begin{cases} (t/\Delta t)^2(3 - 2t/\Delta t) & 0 \le t \le \Delta t \\ 1 & t_1 \le t \le t_2 \\ 1 - 2[(t - t_2)/2\Delta t]^2[3 - 2(t - t_2)/2\Delta t] & t_2 \le t \le t_3 \\ -1 & t_3 \le t \le t_4 \\ -1 + [(t - t_4)/\Delta t]^2[3 - 2(t - t_4)/\Delta t] & t_4 \le t \le T \end{cases} \tag{12}$$

where T denotes the final maneuver time and each indexed time parameter is represented as $\Delta t = t_1 = \alpha T$, $t_2 = T/2 - \alpha T$, $t_3 = T/2 + \alpha T$, and $t_4 = T - \alpha T$. The parameter α ($0 < \alpha < \frac{1}{4}$) is a shaping parameter that determines the smoothness of the shaping action. Note that the smoothed torque profile is also based on the pure rigid-body system of Eq. (11). The shaped torque, when applied to the original flexible dynamics, was shown to be highly effective in reducing vibration energy at the cost of a slight increase in maneuver time.[23] Following application of the shaped torque input into Eq. (11), a useful relationship between the torque level and other parameters is derived as[23]

$$T = \sqrt{\frac{I_{\text{tot}}(\theta_f - \theta_0)}{N\left(\frac{1}{4} - \alpha/2 + \alpha^2/10\right)}} \tag{13}$$

where θ_f and θ_0 are the final and the initial hub angles, respectively. The selection of different design parameters therefore yields other necessary parameters. The reference torque profile is integrated twice to build the reference angle (θ_{ref}) and angular rate ($\dot{\theta}_{\text{ref}}$) histories. A graphical representation of the reference trajectories is provided in Fig. 3.

The feedback tracking control law has been already thoroughly demonstrated in Ref. 23 through analysis and experiment. Because our objective is to derive a control law for on–off thrusters, the tracking control law of Eq. (10) is incorporated into a switching control law. The time-varying control signal in Eq. (10) is now used as an argument of the sign function as

$$u(t) = N \operatorname{sign}[u_{\text{ref}} - g_1(\theta - \theta_{\text{ref}}) - g_2(\dot{\theta} - \dot{\theta}_{\text{ref}})] \tag{14}$$

The inclusion of the tracking control law in the switching function may seem to be a rather ad hoc approach. However, this approach produces a new switching function essentially different from that of the strict minimum-time case. It should be noted that the argument inside sign function in Eq. (14) is sensitive at the early stage of maneuver. The argument lies close to the zero-crossing line around the start of maneuver, and we can expect multiple sign changes of the switching function. This constitutes a significant difference compared with the switching function of Eq. (7) for which the inside argument maintains the same sign until the half-maneuver time because of the constant final angle θ_f.

The early firings by the new switching function are expected to lead to a different switching profile after the half-maneuver time. It is worthwhile to note that there are two additional design parameters (g_1 and g_2) in the tracking control law whereas there is no free design parameter in Eq. (7). The new switching function therefore has some

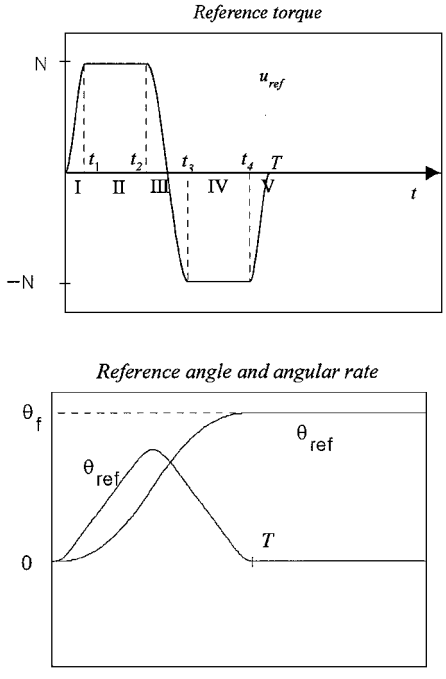

Fig. 3 Graphical representation of reference trajectories.

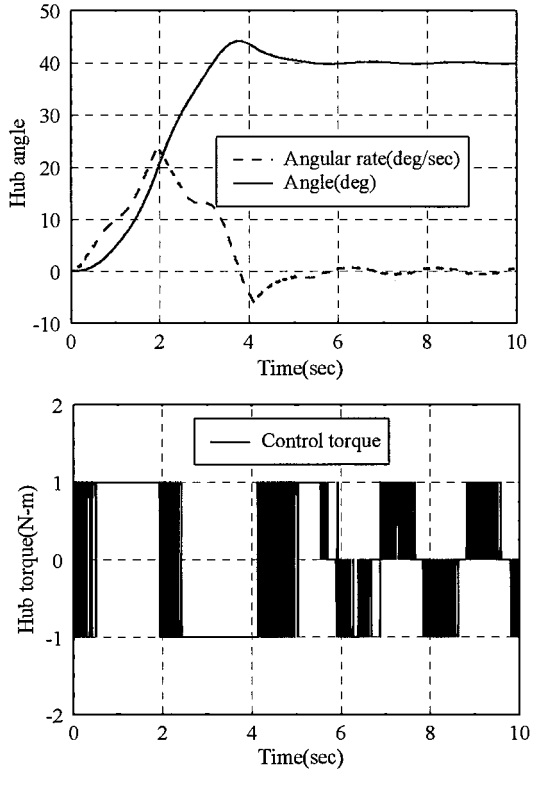

Fig. 4 Simulation results with the on–off switching law based on the closed-loop tracking control law.

flexibility through selection of feedback gains. Note that the original benefit of the smooth reference trajectory in the closed-loop tracking control law is not directly reflected in the on–off feedback switching function. This is due to the discontinuity of the actuator and the sign function with on–off states only. Sample simulation results obtained with the new switching function with a set of feedback gains are presented in Fig. 4. A deadband which consists of a linear combination of absolute values of angle and angular velocity errors is implemented in the simulation.

The hub-angle behavior seems similar to that of Fig. 2, but the control response is somewhat different. The new switching function produces firings at the start of maneuver. Consequently, the half-maneuver time is shifted to the right by the early firings. In this closed-loop switching function control law, the maneuver time is not expressed analytically in terms of the feedback gains (g_1, g_2) because of the nonlinear nature of the sign function and the feedback control law. Because of the multiple switchings in the earlier phase of maneuver, the maneuver time itself tends to increase compared with the pure minimum-time maneuver. Despite the fact that there is not much improvement in the hub-angle response, there still exists some room for improvement with different design parameter sets (g_1, g_2). It should be noted again that the original smoothing effect with continuously varying control output is not reflected in the switching function for thrusters. This raises a need for modulation of the thruster output to reconstruct the continuous shaped torque history in Sec. IV.

IV. Modulation of Continuous Signal

In Sec. III, the shaped reference torque profile and associated reference trajectories are used to build a new feedback switching function. However, because of the characteristic of the sign function, the smoothing effect is not reflected in the actuator output. The switching function decides on–off states only. Thus the modulation technique is adopted for the on–off actuator output. The PWM is applied to the discrete actuator output to construct the equivalent continuous output. The switching function as a reference trajectory developed by the tracking control law is taken as an input to the modulator whose output duration is proportional to the magnitude of input. The pulse width is adjusted at a constant sampling period for the PWM technique.

For application of PWM to the tracking control law, we first take note of the shaped torque profile in Fig. 3. The reference torque input consists of five intervals (I–V). Let us consider interval I for which the shaping function is given in Eq. (12) as

$$f(t) = (t/\Delta t)^2(3 - 2t/\Delta t) \tag{15}$$

Now we discretize the preceding shaping function as in Fig. 5 into n discrete segments. Each segment has different duration of output at the regular sampling period (T_s).

To apply PWM, the shaping function is now transformed into a new function whose output corresponds to the thruster pulse width. Let us consider the maximum pulse width $\delta_{\max}$ achieved at the end of the first maneuver, as the control torque starts from zero, reaching a maximum at $t = \Delta t$. Then the new shaping function for PWM becomes

$$\tilde{f}(t) = \delta_{\max}(t/\Delta t)^2(3 - 2t/\Delta t) \tag{16}$$

Note that the maximum of $\tilde{f}$ is $\delta_{\max}$ because the maximum value of $f(t)$ is equal to 1. The pulse width equal to the sampling period corresponds to the continuous thruster firing. It should be noted that the new shaping function $\tilde{f}$ has the unit of time that determines the

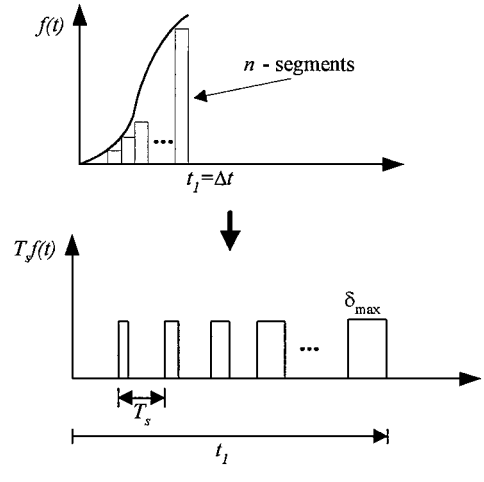

Fig. 5 Discretization of the smoothed trajectory into n segments.

pulse width of the signal. It needs to be reminded that the goal of PWM in the first interval is to build a torque profile close to the original smoothed trajectory to the extent possible.

The design parameters of the PWM now are sampling period T_s and the maximum pulse width $\delta_{\max}$. To determine them, we try to match the momentum imparted by different control inputs. First, the integral of the original shaping function over interval I, which is equivalent to the angular momentum normalized by the thruster level, becomes

$$J = \int_0^{\Delta t} f(t)\,\mathrm{d}t = \int_0^{\Delta t} \left(\frac{t}{\Delta t}\right)^2 \left(3 - \frac{2t}{\Delta t}\right) \mathrm{d}t = \frac{1}{2}\Delta t \tag{17}$$

On the other hand, the PWM output signal represents a series of pulse durations of each interval, which is determined by the current time. In other words, $\tilde{f}(iT_s)$ is the pulse duration of the ith discretized segment in Fig. 5. Therefore, the net pulse duration can be obtained if a summation is taken over n segments as

$$\sum_{i=1}^{n} \tilde{f}(iT_s) = \sum_{i=1}^{n} \delta_{\max} \left(\frac{iT_s}{\Delta t}\right)^2 \left(3 - 2\frac{iT_s}{\Delta t}\right) \tag{18}$$

From a mathematics handbook the above series expression is expanded as

$$\sum_{i=1}^{n} \tilde{f}(iT_s) = \delta_{\max} \frac{T_s^2}{\Delta t^2} \left[3\frac{n(n+1)(2n+1)}{6} - 2\frac{T_s}{\Delta t}\frac{n^2(n+1)^2}{4}\right] \tag{19}$$

Let us note that the maneuver interval is divided into n equal segments. Thus we have the following relationship:

$$\Delta t = nT_s \tag{20}$$

By using the preceding relationship, we can rewrite Eq. (19) as

$$\sum_{i=1}^{n} \tilde{f}(iT_s) = \delta_{\max} \frac{1}{n^2}\frac{1}{2}[n(n+1)(2n+1) - n(n+1)^2] = \frac{1}{2}\delta_{\max}(1+n) \tag{21}$$

Equation (21) thus represents a quantity similar to that of Eq. (17) by conversion into the PWM of the continuous signal. Next, to equate the result of integral in Eq. (17) with that of Eq. (21), the following equality needs to be satisfied:

$$\delta_{\max}(n+1) = \Delta t \tag{22}$$

In other words,

$$\delta_{\max} = \Delta t/(n+1) \tag{23}$$

The physical interpretation of Eq. (23) is the maximum pulse width that produces the first area integral by PWM equal to that of the continuous trajectory over the first interval of maneuver. It is noteworthy that $\delta_{\max}$ becomes small if n becomes large, and this is a natural tendency with the increasing number of firings. Also, Eq. (23) can be rewritten in terms of sampling period T_s. Thus we have only one design parameter that automatically determines the other parameter. For instance, T_s determines n from Eq. (20), which yields $\delta_{\max}$ in Eq. (23).

Note that the second interval (II) maintains the maximum torque level. The PWM technique now blends into a constant pulse-width control over the second interval. This results in continuous firing of thrusters with the pulse width equal to the sampling period with $\delta_{\max} = T_s$. Note that over the third interval (III) the continuous smoothing function is given as

$$f(t) = 1 - 2[(t - t_2)/2\Delta t]^2[3 - 2(t - t_2)/2\Delta t] \tag{24}$$

and the new smoothing function is redefined as

$$\tilde{f}(t) = \delta_{\max} f(t) \tag{25}$$

The area integral obtained with the original smoothing function becomes zero because of the symmetry of the torque profile about the half-maneuver time. The discretized pulse-width function has the similar property because

$$\sum_{i=n}^{1} \tilde{f}(iT_s) + \sum_{i=1}^{n} \tilde{f}(iT_s) = 0 \tag{26}$$

where the first term corresponds to the maneuver left to the half-maneuver time and the second term corresponds to the right-hand side of the half maneuver. Now intervals IV and V are basically identical to intervals II and I, respectively, except for the sign reversal in the control torque. The thruster output is constant over interval IV while the PWM technique is applied over the interval V. In summary, the PWM of the shaped torque profile over the whole maneuver phase can be rewritten as

$$\tilde{f}(iT_s) = \begin{cases} \delta_{\max} f(iT_s) & 0 \le t \le \Delta t \\ T_s & t_1 \le t \le t_2 \\ \delta_{\max} f(iT_s) & t_2 \le t \le t_3 \\ -T_s & t_3 \le t \le t_4 \\ \delta_{\max} f(iT_s) & t_4 \le t \le T \end{cases} \tag{27}$$

Hub-angle responses by the PWM technique based on the shaped torque profile and the strict minimum-time torque input with a single switching at the half-maneuver time are presented in Fig. 6. In this simulation the shaping parameter is set equal to 0.1 and the sampling period T_s is selected as 0.02 s.

In Fig. 6 we can see that the open-loop control torque by PWM of the shaped torque results in less overshoot compared with Fig. 2. The modulated thruster output effectively contributes to reducing the overshoot as well as to reducing residual vibration compared with the strict minimum-time case. The peak-to-peak variation by the strict minimum-time input is more severe than the PWM case. More dominant trends are expected when the control torque level is increased. Also, in Fig. 6 there is a slight offset in hub-angle response by the modulated pulse input. This is due to the finite discretization and/or error in the applied torque. The design parameters are decided by matching the first integral of the torque input. The discrepancy in the final angular displacement is expected therefore because the angle response is the double-time integral of the torque input. The offset problem can be solved by a feedback control law to be discussed in the section on feedback switching control.

The analysis conducted so far is for the one shaping function case in Ref. 23. It should be noted that other types of smoothing functions may lead to similar results. That is, the PWM technique can be combined with wide classes of time-varying shaping functions to produce a derived smoothing torque profile for on–off actuators. The performance of PWM is obviously dependent on the design parameters such as sampling time and/or maximum pulse width.

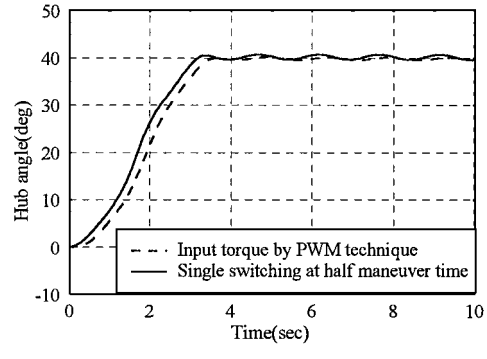

Fig. 6 Hub-angle response by the pulse-width-modulated shaped torque profile (case I) and simple minimum-time strategy with one switching (case II).

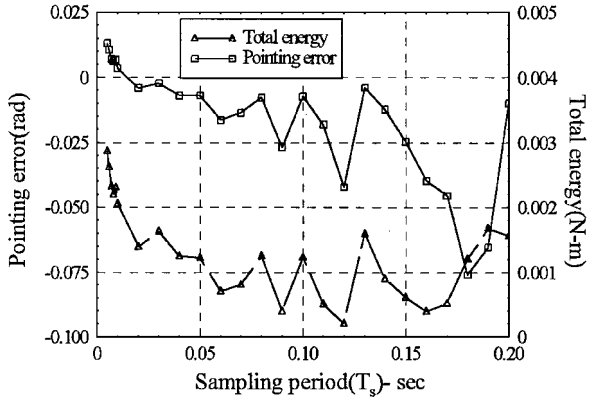

Fig. 7 Vibrational energy at the end maneuver over the varying sampling periods.

Update Interval

The sampling period (frequency) is an important design parameter in PWM. It implicitly decides the behavior of the whole flexible dynamics through the modulation of the reference torque based on the pure rigid dynamics. The rule of thumb is to select a moderately high sampling frequency that is a few times higher than the lowest natural frequency of the structure. However, the pointing performance is also dependent on the sampling period because of the error in deciding the parameter by the first time integral.

Figure 7 shows the total vibration energy and the pointing error between the desired hub angle and the actual hub angle at the end maneuver ($t = T$) vs the sampling period changes.

As can be seen in Fig. 7, the vibration energy level decreases with increasing sampling period in general, except for some oscillatory regions. This indicates that the longer sampling period or smaller number of impulsive inputs leads to less vibration. However, the pointing performance is improved by a shorter sampling period. Thus the selection of sampling period should be made based on a tradeoff between the pointing performance and vibration by the pure open-loop pulse input.

Feedback Switching Control

Modulation of the continuous near-minimum-time torque shaping function was introduced in the preceding section to build an open-loop control command. Because of the finite discretization error, offset pointing error was observed in the simulation results. There are also other potential error sources such as external disturbances as well as modeling errors from the pure rigid dynamics. For consideration of practical issues, the open-loop PWM approach is further extended into a feedback switching strategy. This idea is implemented by use of the continuous version of the tracking control law of Eq. (10). From Eq. (10) the original feedback tracking control law is used to produce a new normalized switching function $\xi(t)$ as

$$\xi(t) = f(t, \Delta t) - [g_1(\theta - \theta_{\text{ref}}) + g_2(\dot{\theta} - \dot{\theta}_{\text{ref}})]/N \qquad (28)$$

As a consequence, the final expression of the new closed-loop PWM function becomes

$$\begin{aligned} \tilde{f} &= \delta_{\max}\xi(t) \\ &= \delta_{\max}\{f(t, \Delta t) - [g_1(\theta - \theta_{\text{ref}}) + g_2(\dot{\theta} - \dot{\theta}_{\text{ref}})]/N\} \\ &= \delta_{\max} f(t, \Delta t) + \Delta\delta(t) \end{aligned} \qquad (29)$$

The closed-loop pulse width therefore consists of a linear combination of the open-loop term $[\delta_{\max} f(t, \Delta t)]$ and a correction term $(\Delta\delta)$ by the feedback strategy. The preceding feedback PWM is applied throughout the whole intervals. The pulse width is therefore not constant in any interval by the feedback law. The feedback PWM of the switching function is used for simulation, and the results are plotted in Fig. 8. For comparison purposes, the open-loop response is also plotted.

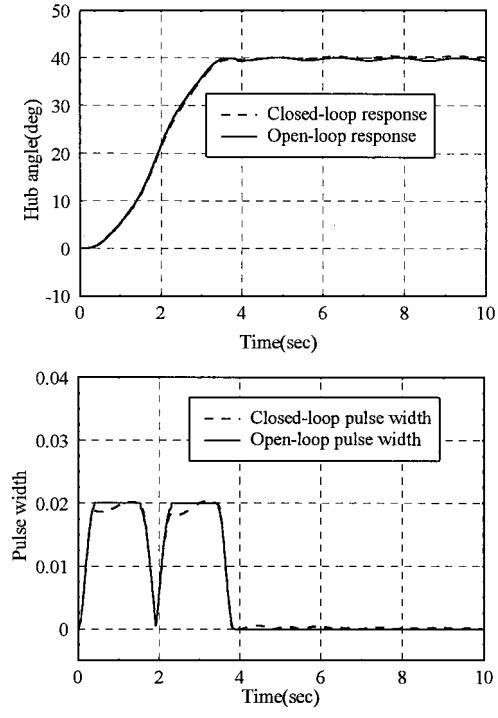

Fig. 8 Open-loop and closed-loop switching-function-based hub angle and pulse-width responses.

As expected, the closed-loop strategy improves the performance of the open-loop response by reaching a steady hub angle. The overall behavior of hub-angle response exceeds that of Fig. 2, proving the advantages of the proposed strategy—a closed-loop switching function with the PWM technique.

Gain Selection

The gain selection in the feedback control approach is important in the sense that the closed-loop switching function is rather sensitive to the feedback gains. This is because the maximum open-loop pulse width is $\delta_{\max}$, whereas the closed-loop correction term is determined by the feedback gains g_1 and g_2. The correction pulse width should be limited to a certain range over the maneuver interval $0 \le t \le T$ by appropriate ranges of feedback gains. Too-small values of feedback gains in turn result in a poor pointing performance after the maneuver $t > T$, in which only the feedback control signal is activated. Thus the gain selection process is not straightforward compared with that of the continuous feedback control case, in which the gain selection can be made without particular constraints on the magnitude.[23] In the continuous feedback case, the feedback gains are required to satisfy only the Lyapunov stability condition.[23] The performance is mainly subject to the smoothed open-loop control input for the continuous feedback tracking control case.

The final pulse width should not possibly exceed the sampling period for desired performance to be achieved. If this situation arises, the output pulse width is set equal to the sampling period. This is similar to the maximum saturation limit of actuator types with continuous output capability. It should be also noted that the sampling period now could become an additional design parameter. In Fig. 8 the sampling period is set equal to 0.02 s, and we can see some areas in which the closed-loop pulse width ($\tilde{f}$) exceeds the sampling period.

V. Conclusion

The closed-loop minimum-time switching function control law based on rigid-body approximation for the slew maneuver of flexible structures may not be appropriate for structure models with dominant flexibility. The multiple firings at the half maneuver time cause the excessive overshoot of angle response. The multiple firings can be shifted if a feedback tracking control law is used as a switching function with free design parameters. The on–off nature of the actuators was shown to be effectively handled by the

pulse-width modulation technique. The smoothed torque profile is used to produce a modulated thruster pulse width in such a way that the resultant output pulse simulates the original continuous torque profile. The open-loop approach was transformed into a closed-loop switching control law to improve the postmaneuver pointing performance. The smoothed torque profile, which is adopted as a reference trajectory in this study, may be replaced, for potential performance improvement, with other optimal reference trajectories. Future experimental verification may add practical merit of the proposed strategy in this study. The actuator wear that might be caused by excessive thruster firings needs to be taken into account for the practical implementation of the approach proposed in this study.

References

[1]Markley, F. L., "Large Angle Maneuver Strategies for Flexible Spacecraft," *Advances in Astronautical Sciences,* Paper AAS 79-156, 1979, pp. 625–647.

[2]Farrenkopf, R. L., "Optimal Open Loop Maneuver Profiles for Flexible Spacecraft," *Journal of Guidance and Control*, Vol. 2, No. 6, 1979, pp. 491–498.

[3]D'Amario, L. A., and Stubbs, G. S., "A New Single-Rotation Axis Autopilot for Rapid Spacecraft Attitude Maneuvers," *Journal of Guidance and Control*, Vol. 2, No. 4, 1979, pp. 339–346.

[4]Swigert, C. J., "Shaped Torque Techniques," *Journal of Guidance and Control*, Vol. 3, No. 5, 1980, pp. 460–467.

[5]Turner, J. D., and Junkins, J. L., "Optimal Large Angle Single Axis Rotational of Flexible Satellites," *Journal of Guidance and Control*, Vol. 3, No. 6, 1980, pp. 460–467.

[6]Breakwell, J. A., "Optimal Feedback Control of Flexible Spacecraft," *Journal of Guidance and Control*, Vol. 4, No. 5, 1981, pp. 427–429.

[7]Vander Velde, W. E., and He, J., "Design of Space Structure Control Systems Using On–Off Thrusters," *Journal of Guidance, Control, and Dynamics*, Vol. 6, No. 1, 1983, pp. 53–60.

[8]Skaar, S. B., Tang, L., and Yalda-Mooshabad, Y., "On–Off Attitude Control of Flexible Satellites," *Journal of Guidance, Control, and Dynamics*, Vol. 9, No. 4, 1986, pp. 507–510.

[9]Singh, G., Kabamba, P. T., and McClamroch, N. H., "Planar Time Optimal, Rest-to-Rest Slewing Maneuvers of Flexible Spacecraft," *Journal of Guidance, Control, and Dynamics*, Vol. 12, No. 1, 1989, pp. 71–81.

[10]Liu, Q., and Wie, B., "Robust Time-Optimal Control of Uncertain Flexible Spacecraft," *Journal of Guidance, Control, and Dynamics*, Vol. 15, No. 3, 1992, pp. 597–604.

[11]Wie, B., Sinha, R., and Liu, Q., "Robust Time-Optimal Control of Uncertain Structural Dynamic Systems," *Journal of Guidance, Control, and Dynamics*, Vol. 15, No. 5, 1993, pp. 980–983.

[12]Singh, T., and Vadali, S. R., "Robust Time-Optimal Control: A Frequency Domain Approach," *Journal of Guidance, Control, and Dynamics*, Vol. 17, No. 2, 1994, pp. 346–353.

[13]Wie, B., Sinha, R., Sunk el, J., and Cox, K., "Robust Fuel- and Time-Optimal Control of Uncertain Flexible Space Structures," *AIAA Guidance, Navigation, and Control Conference*, AIAA-93-3804-CP, AIAA, Washington, DC, 1993, pp. 939–948.

[14]Banerjee, A. K., "Dynamics and Control of the Shuttle-Antennae System," *Journal of the Astronautical Sciences*, Vol. 41, No. 1, 1993, pp. 73–90.

[15]Singhose, W., Banerjee, A. K., and Seering, W., "Slewing Flexible Spacecraft with Deflection Limiting Input Shaping," *Journal of Guidance, Control, and Dynamics*, Vol. 20, No. 2, 1997, pp. 291–298.

[16]Singhose, W. E., Mills, B. W., and Seering, W. P., "Closed-Form Methods for On–Off Control of Multi-Mode Flexible Structures," *IEEE Conference on Decision and Control*, Inst. of Electrical and Electronics Engineers, New York, 1997, pp. 1381–1386.

[17]Singh, T., "Fuel/Time Optimal Control of the Benchmark Problem," *Journal of Guidance, Control, and Dynamics*, Vol. 18, No. 6, 1995, pp. 1225–1231.

[18]Singhose, W., Bohlke, K., and Seering, W., "Fuel-Efficient Pulse Command Profiles for Flexible Spacecraft," *Journal of Guidance, Control, and Dynamics*, Vol. 19, No. 4, 1996, pp. 954–960.

[19]Hablani, H. B., "Zero-Residual-Energy, Single-Axis Slew of Flexible Spacecraft Using Thrusters: Dynamics Approach," *Journal of Guidance, Control, and Dynamics*, Vol. 15, No. 1, 1992, pp. 104–113.

[20]Agrawal, B. N., and Bang, H., "Robust Closed-Loop Control Design for Spacecraft Maneuver Using On–Off Thrusters," *Journal of Guidance, Control, and Dynamics*, Vol. 18, No. 6, 1995, pp. 1336–1349.

[21]Byers, R. M., Vadali, S. R., and Junkins, J. L., "Near-Minimum Time, Closed-Loop Slewing of Flexible Spacecraft," *Journal of Guidance, Control, and Dynamics*, Vol. 13, No. 1, 1990, pp. 57–65.

[22]Fuji, H., Ohtsuka, T., and Udou, S., "Mission Function Control for Slew Maneuver Experiment," *Journal of Guidance, Control, and Dynamics*, Vol. 12, No. 6, 1989, pp. 858–865.

[23]Junkins, J. L., Rahman, Z., Bang, H., and Hecht, N., "Near-Minimum-Time Control of Distributed Parameter Systems: Analytical and Experimental Results," *Journal of Guidance, Control, and Dynamics*, Vol. 14, No. 2, 1991, pp. 406–415.

[24]Athans, M., and Falb, P. L., *Optimal Control—An Introduction to the Theory and Its Applications*, McGraw–Hill, New York, 1966, pp. 364–503.